Conformational Effects of Calcium Release from Parvalbumin: Comparison of Computational Simulations with Spectroscopic Investigations†

Monique Laberge, Wayne W. Wright, Katakam Sudhakar, Paul A. Liebman, and Jane M. Vanderkooi*

Johnson Research Foundation, Department of Biochemistry and Biophysics, School of Medicine, University of Pennsylvania, Philadelphia, Pennsylvania 19104

Received September 27, 1996; Revised Manuscript Received February 7, 1997⊗

ABSTRACT: The effect of Ca^{2+} binding to parvalbumin was monitored by probes of conformation including absorption, fluorescence, circular dichroism (CD), infrared (IR) spectroscopy and differential scanning calorimetry. These experimental studies were compared with molecular dynamics computations on the structures of the Ca-bound and Ca-free forms of cod parvalbumin. The UV CD spectra show that removal of calcium results in a decrease in the α-helical content of the protein. The IR amide I′ and III′ regions are very much affected by Ca removal and are indicative of significant perturbation of secondary structure. The fluorescence of tryptophan, the IR markers, and UV ellipticity all show changes with temperature, pointing to a lowering of protein stability upon Ca removal. These results are consistent with the structures obtained for both the Ca-bound and Ca-free proteins after 200 ps of solvated molecular dynamics simulations which show a decrease in the secondary structure upon Ca removal.

From common thermodynamic considerations, it is clear that the binding of a substrate, cofactor, or metal to a protein will generally increase its stability since the unfolding energy would now include an additional penalty for breaking favorable ligand or metal interactions—assuming that the ligand or metal affinity is lower in the unfolded state. In fact, there are many examples showing how the binding of metals or cofactors to proteins increases protein stability and the structural compactness of proteins. A textbook model is hexokinase in which the binding of the substrate glucose results in a more compact form (Anderson et al., 1979). Another example is of clinical importance: for some patients with propionyl-CoA carboxylase deficiency, administration of megadoses of the cofactor biotin relieves some of the clinical manifestations, presumably because the cofactor stabilizes the defective enzyme and therefore increases its *in vivo* stability (Barnes et al., 1970). Stabilization of protein folding by cations and anions has been established quantitatively for several protein systems (Pace & Grimsley, 1988; Sugawara et al., 1991), and for some others, cofactors are required for folding (Jaenicke, 1987). Conversely, when the ligand binds tighter to the unfolded form, then its binding will destabilize the protein. The classic example results in the T−R transition in hemoglobin upon oxygen binding.

In view of the role of Ca^{2+} in regulating cellular processes in all organisms (Gerday et al., 1988), the effect of calcium binding on protein structure is an important subset of the general topic of how ligand interactions affect protein structure. Ca-binding proteins have been shown to recognize Ca^{2+} ions and to bind them with great affinity while readjusting their conformations to carry out essential biological functions that are in turn involved in the regulation of other enzymatic processes. The conformational changes elicited by calcium have been studied in many Ca-binding proteins, and in this work, we are using cod fish muscle parvalbumin isotype III as a representative Ca-binding protein. Parvalbumins, found in vertebrates, are small (M_w ∼11 500, ∼108 amino acids) globular proteins that bind Ca^{2+} and Mg^{2+} ions (Declercq et al., 1991). They are thought to be active either in Ca transport or as intracellular Ca buffers in certain excitatory cells, shuttling Ca^{2+} in fast muscle fibers back to the sarcoplasmic reticulum (Celio, 1990). The structures of some 40 parvalbumins are known, either from sequence analysis or NMR and X-ray structure determination. Only cod and whiting parvalbumins have a single Trp in their amino acid sequences (Hutnik et al., 1990), which makes them ideally suited for assessing the spectroscopic role of Trp. The X-ray structures show that the structure of the Ca-bound form is conserved from various sources over a wide phylogenetic range, all of them having six α-helical regions labeled A−F (or 1−6) and no disulfides (Henrickson & Karle, 1973; Kretsinger & Nockolds, 1973; Kumar et al., 1990; Declercq et al., 1991; Roquet et al., 1992). There are two regions in the protein associated with each of the two Ca^{2+}-binding sites (Figure 1). The EF Ca-binding site consists of the E and F helices and a connecting loop with a Ca-binding site. The second domain contains the second binding site for Ca^{2+} and is formed by the C and D helices connected by another loop. The A and B helices form the central core of the protein. The Ca-free form has not yet been crystallized.

The structural information derived from molecular dynamics now represents a solid basis for experimental research, and molecular simulations are increasingly used to complement experimental data and refine structural details. Computational simulations on other Ca-binding proteins, namely, calmodulin, troponin C, and calbindin, have yielded a wealth of information concerning the role of calcium in triggering significant conformational and functional changes in these proteins (Mehler et al., 1991, 1993). Here we examine how

†This work was supported by National Institutes of Health Grants GM 34448, PO1 GM48130, EY00012, and EY01583.

* Author to whom correspondence should be addressed. Fax: 215-573-2042. Phone: 215-898-8783. E-mail: vanderko@mail.med.upenn.edu.

⊗ Abstract published in *Advance ACS Abstracts,* April 15, 1997.

S0006-2960(96)02436-1 CCC: $14.00

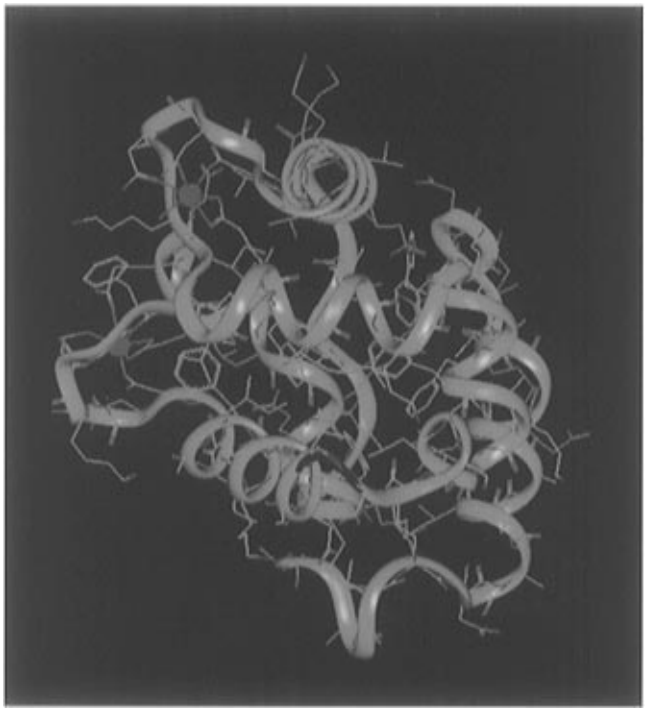

FIGURE 1: Three-dimensional view of the six-helical cod parvalbumin modeled from the X-ray structure of carp parvalbumin. The two spheres in purple represent the two calcium atoms bound respectively to Asp92 (OD1), Glu101 (OE2 and OE1), Asp94 (OD1), Ala96 (O), Wat166 (O), and Asp 90 (OD2) and to Phe57 (O), Asp51 (OD1), Glu62 (OE1 and OE2), Asp53 (OD1), Ser55-(OG), and Glu59(OE1).

a combination of spectroscopic techniques (FTIR, CD,[1] and fluorescence) can detect the calcium-induced conformational change and we compare these observations with structural indications obtained from molecular dynamics simulations (MDS) of both the Ca-bound and Ca-free cod parvalbumins. Although the structure of the Ca-bound parvalbumin is known, the structure of the Ca-free protein is not; it has been suggested that the Ca-free species is somewhat like a "molten globule" with perhaps some structured regions (Jackson et al., 1991; Sudhakar et al., 1995) and, in this context, the calcium-depleted simulations are of interest.

EXPERIMENTAL PROCEDURES

Materials. Guanidine hydrochloride (GdnHCl) and Chelex 100 were obtained from Sigma Chemical Co. (St. Louis, MO). Other chemicals were of the highest purity that was commercially available. Water was passed over an ion-exchange resin and then glass distilled. Parvalbumin type III was prepared from frozen cod (*Gadus callarius L*) fillets, obtained from a local fish market using a procedure (Sudhakar et al., 1993a) that uses small modifications of published procedures (Haiech et al., 1979; Horrocks & Collier, 1981). For all measurements, the protein was dissolved in 10 mM sodium phosphate and 0.1 M NaCl, pH 7.0. No additional calcium was added to the Ca-bound protein, and the free Ca^{2+} can be estimated to be $\sim 10^{-5}$ M [this value is obtained from Ca and EDTA titration curves (Sudhakar et al., 1995)]. For the Ca-free protein Ca was removed from the protein by passage over a Chelex column of 10 cm length and/or by adding EGTA or EDTA. Since these procedures do not necessarily decrease the Ca^{2+} levels below saturation levels (Hutnik et al., 1990), Ca removal and the fractional Ca saturation were ascertained by the shift in the fluorescence spectrum (Sudhakar et al., 1995).

Spectroscopy. Absorption spectra were recorded on a Hitachi U3000 spectrometer. Steady-state fluorescence spectra were recorded with a Perkin-Elmer 650 10S spectrometer.

Circular dichroism (CD) spectra were acquired with an Aviv 62DS circular dichroism spectrophotometer. Ellipticities, θ, expressed in deg cm^2 dmol^{-1}, were normalized to residue concentration using the relationship

$$\theta = \theta_o/(lcN) \quad (1)$$

where θ_o is the observed ellipticity, l is the path length of the cell (in mm), c is the molar concentration of protein, and N is the total number of residues in the protein.

A Bruker IFS 66 FTIR spectrometer equipped with a Globar source, a KBr beam splitter, and a MCT detector was used for infrared (IR) measurements. The sample holder had CaF_2 windows and its path length was 50 μm. The temperature of the sample was controlled to within 0.5 °C with a circulation bath. The data were acquired with a four-point apodization function at a resolution of 2 cm^{-1}. For the mid-IR region, lyophilized parvalbumin was dissolved in D_2O buffer and the sample allowed to sit for about 1 h at room temperature before measurement was initiated.

Differential Scanning Calorimetry. Differential scanning calorimetry (DSC) measurements were done with a Microcal Inc. microcalorimetry system (Lowell, MA). The Origin DSCAnalytic software from MicroCal Inc. was used for analysis.

Molecular Dynamics. For the MDS, the starting structure of carp parvalbumin was obtained from the Brookhaven Protein Data Bank (Bernstein et al., 1977), pdb4cpv.ent (Kumar et al., 1990). The amino acid sequence of the carp structure was modified to include the 20 amino acid residues known to be present in cod parvalbumin by sequence analysis (Hutnik et al., 1990), namely, Ala88, Gly89, Asp90, Ser91, Asp92, Gly93, Asp94, Gly95, Ala96, Ile97, Gly98, Val99, Asp100, Glu101, Trp102, Ala103, Val104, Leu105, Val106, and Lys107 using the Biopolymer module of the InsightII software package (Molecular Simulations, Inc., San Diego, CA) on a Silicon Graphics IRIS Indigo2 workstation. The molecular dynamics were performed using the Discover–3 software package (Molecular Simulations, Inc., San Diego, CA) with the cvff91 force field (Hagler et al., 1974; Hagler & Lifson, 1974) and repeated with the ESFF force field. Calcium parameters were taken from the literature (Hori et al., 1988) and incorporated into ESFF with optimization of the two Ca-binding sites present in cod parvalbumin, i.e., sites EF and CD. Table 1 lists the parameters thus obtained. Simulations were carried out on both Ca-bound and Ca-free parvalbumins. To remove artifacts due to the addition of explicit hydrogens, the initial structures were minimized using a steepest descent algorithm until the rms derivative reached 0.1 kcal mol^{-1} and then subjected to 2000 conjugate gradient iterations. Two types of simulations were carried out: a first 120-ps series, in which the bulk effect of the solvent was modeled using the distance-dependent dielectric

[1] Abbreviations: CD, circular dichroism; DSC, differential scanning calorimetry; IR, infrared; EDTA, ethylenediaminetetraacetate; EGTA, ethylene glycol bis(β-aminoethyl ether)-*N*,*N*,*N*′,*N*′-tetraacetate; MDS, molecular dynamics simulation.

Table 1: Calcium Parameters

bond atom types[a]	bond energy[b]	α[b]
O′−Ca	93.22377	0.98479
O−Ca	94.22449	0.97534
Oa−Ca	93.63089	0.97153
angle atom types[a]	**force constant[c]**	**θ_0**
C═O′−Ca	68.20201	123.93975
C−O−Ca	57.38286	132.62842
C═Oa−Ca	68.64707	121.91409
O′−Ca−O′	39.79995	81.81340
O′−Ca−Oa	42.31822	92.77542
torsion angle	**force constant[c]**	**no. of angles**
Ca−C−C═O′	0.10422	1
Ca−C−C═H	0.20844	1
H*−Ca−C═C	0.23688	2
Ca−C−C−CP	0.15806	1
Ca−C−C−C	0.15806	2

[a] As defined in the ESFF force field (InsightII−Discover_3 User Manual). [b] In kcal mol^{-1}. In ESFF, a Morse function is used for bond energy calculations and α is an anharmonicity parameter. [c] In kcal mol^{-1} Å^{-2}.

approximation (Harvey, 1989; Mehler, 1990; Solmajer & Mehler, 1991). The dielectric constant, ϵ, was set to 1, retaining the waters of the X-ray structure. The second series was performed on fully solvated Ca-free and Ca-bound parvalbumins using a constant dielectric of 1. The proteins were solvated in a perodic boundary cell of 37 Å^3 to generate bulk solvent (1205 waters). The 3D solvent cell was equilibrated, holding the protein's coordinates fixed, and then the whole solvated system was subjected to conjugate gradient minimization, followed by the dynamics simulations which were carried out at a constant temperature of 300 K using a leapfrog algorithm with a time step of 1 fs. Nonbond interactions were taken into account using the cell multipole method (Schmidt & Lee, 1991; Ding et al., 1992) as implemented in the Discover_3 software package. This method offers the advantage of being more rigorous and efficient than the application of cutoffs. Relatively recent in its application, the cell multipole method allows calculation of both near-field and far-field interactions, the former due to the surrounding atoms and the latter due to the rest of the ensemble atoms. The number of near-field interactions is easy to calculate since they are relatively limited. On the other hand, the number of interactions in the far field scale as N^2, making it very hard to compute accurately for large ensembles. The cell multipole approach does this by representing the potential associated with each basic cell as a general potential located in the center of the cell which it then expands into an infinite series of multipole moments; the far-field potentials are obtained by summing all the far-field contributions. The resulting potential can then be expanded as a Taylor series, using a hierarchical method. As such, it is an "order N" method, and significant CPU time savings can be achieved when compared to using an exact N^2 algorithm (Ding et al., 1992). The system was brought to 300 K over 20 ps, and dynamics were run for 200 ps.

RESULTS

Spectral Changes with Ca Binding. The UV absorption spectra of cod parvalbumin are presented in Figure 2A. The

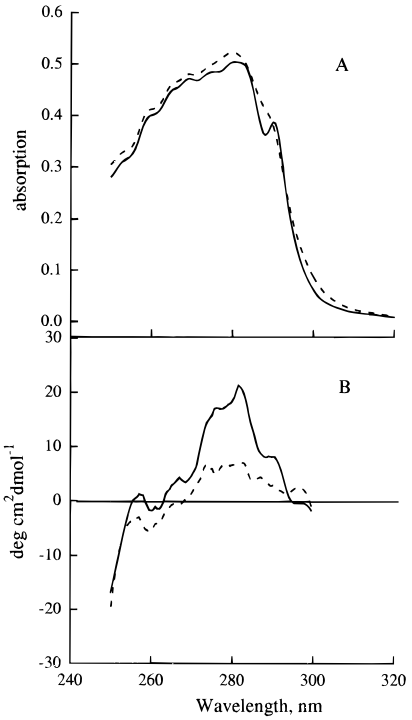

FIGURE 2: (A) Absorption spectra of Ca-free parvalbumin (dashed line) and Ca-bound parvalbumin (solid line). The concentration of the protein was 1.1 mM in 0.01 M phosphate and 0.1 M NaCl at pH 7.0. Temperature: 20 °C. Cell path length: 1 mm. (B) Near-UV CD spectrum of parvalbumin in the presence (solid line) and absence (dashed line) of Ca. Protein concentration: 1.1 mM. The temperature was maintained at 25 °C. Ca removal was achieved by addition of EDTA as described in Materials and Methods. The band-pass was 1 nm, the step size was 0.5 nm, and the accumulation time per data point was 5 s. Cell path length: 1 mm.

spectrum in the presence of Ca shows the characteristic resolved spectrum of indole in a hydrophobic solvent (Longworth, 1971). Since cod parvalbumin contains no Tyr and a single Trp at position 102, the spectrum reflects environmental changes at the single Trp site. The Frank−Condon-active vibrational bands of the L_b are observed at 260, 268, 272, 275, 284, and 292 nm (Callis, 1991). The effect of Ca removal is significant: the spectrum broadens, resulting in loss of vibrational resolution, in agreement with other reports. (Horrocks & Collier, 1981). These spectral changes in the presence of calcium are indicative of a change in the chromophore electronic structure reflecting a more compact, apolar and hydrophobic environment for Trp102 (Persson & Petersen, 1995).

Due to the large absorption of Trp in this region and the absence of Tyr, the CD spectrum in the near-UV also reports on the Trp environment. As seen in Figure 2B, in the presence of calcium, the spectrum mainly displays positive bands in the L_b transition region above 275 nm. Three vibrational bands are observed at 275, 280, and 293 nm. Calcium removal results in a significant loss of intensity, indicating that the Trp102 environment is perturbed (Strickland et al., 1969).

Figure 3A shows the far-UV CD spectra of both forms of parvalbumin. Their overall appearances are indicative of a high content of α-helical structure, namely, the presence of a positive band at 201 nm (with Ca), shifted to ~199 nm upon Ca removal, and intense negative bands at 207 and 222 nm (Johnson, 1990). As expected, removal of Ca decreases the intensity of the ellipticity but the bands still

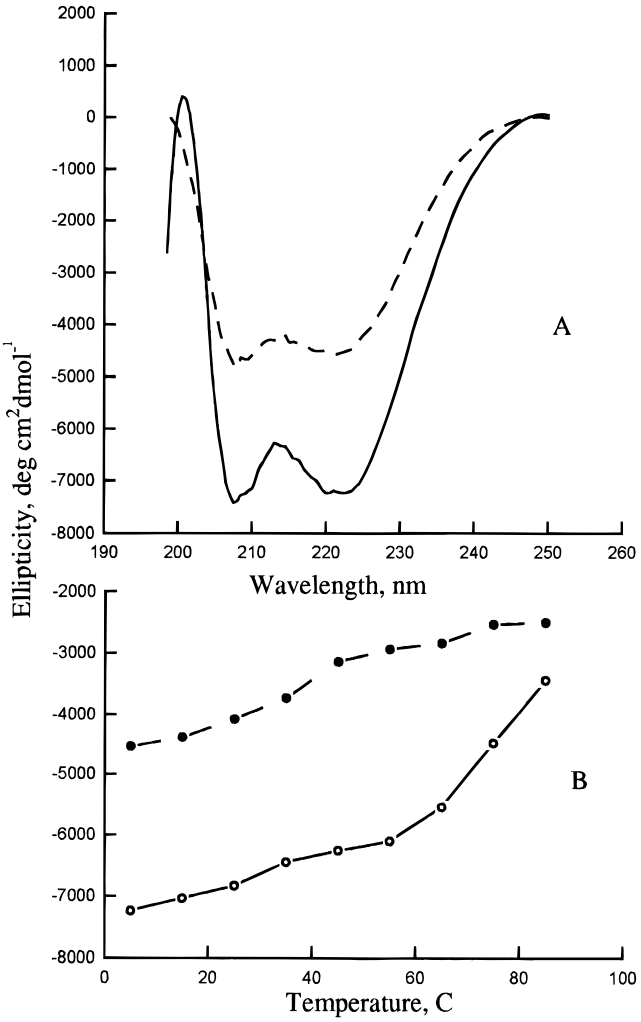

FIGURE 3: (A) Far-UV CD spectrum of parvalbumin in the presence (solid line) and absence (dashed line) of Ca^{2+}. Protein concentration: 45 μM. The temperature was maintained at 5 °C. Buffer conditions are the same as in Figure 2. (B) Ellipticity for the Ca-bound (open circles) and Ca-free (closed circles) parvalbumin at 222 nm.

maintain their α-helical signatures (Eberspach et al., 1988; Kuwajima, 1989; Hutnik et al., 1990).

The temperature dependence of the CD spectra for the Ca-bound and Ca-free parvalbumin was examined. The ellipticity at 222 nm of the Ca-parvalbumin changed at temperatures above 60 °C while the Ca-free protein showed a continuous decrease in ellipticity with temperature rise (Figure 3B).

Changes of Conformation with Ca: DSC. Figure 4 shows the DSC profile for the Ca form of the protein. The DSC data could not be fit to a single two-state model, nor was the fit acceptable using a model in which there were two independent sequential two-state transitions. The smooth curve superimposed on the experimental data shows the calculated best fit by a two-transition non-two-state model. The first transition is observed at 70 °C, and the calorimetric and van't Hoff enthalpies are approximately the same (47 and 54 kcal). The second transition, at 76 °C, yields calorimetric and van't Hoff energies (30 and 76 kcal, respectively). Nonequivalence of the two types of ΔH's is expected for proteins with more than one domain and would also be expected for a protein whose stability depends upon the ligation of two Ca ions (Brandts et al., 1989). Repeated

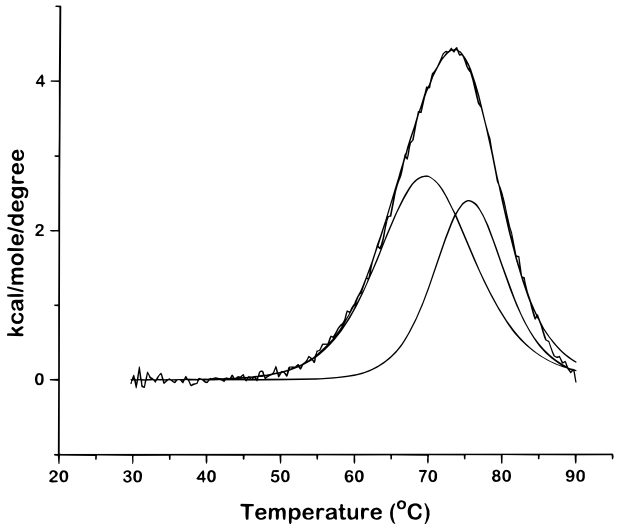

FIGURE 4: Differential scanning calorimetry. The temperature profile is baseline subtracted and concentration normalized. The concentration of the protein used was 90 μM in 0.01 M phosphate and 0.1 M NaCl at pH 7.0. The solid line through the noisy experimental data is the computer fit using these parameters: first transition temperature T_{m1} = 69.7 °C, ΔH = 47 kcal, and van't Hoff energy = 54 kcal; second transition temperature T_{m2} = 76 °C, ΔH = 30 kcal, and van't Hoff energy = 76 kcal/mol.

scans showed the same temperature transition (while showing some loss of intensity due to irreversible heat denaturation of the sample). The parvalbumin from carp has previously been reported to have thermal transition properties inconsistent with a two-state model with a transition temperature of 90 °C in the presence of 10^{-4} M Ca (Filimonov et al., 1978).

DSC was also attempted on the Ca-free protein. In the absence of Ca, the protein did not show a sharp thermal denaturation profile, and DSC scans could not be reliably analyzed above background thermal changes of the buffer at the available protein concentrations (data not shown).

Temperature Dependence of Fluorescence. It was previously reported (Permyakov et al., 1983; Castelli et al., 1988; Eftink & Wasylewski, 1989) that there are large red shifts in the Trp emission maximum when Ca is removed. The emission spectra for the Ca protein as a function of temperature are summarized in Figure 5, and the intensity of fluorescence for the Ca^{2+}-bound, partially bound, and free proteins is given in the inset. For the Ca-bound protein, the intensity is relatively constant from 10 to 40 °C; above 40 °C the intensity decreases with temperature increase, indicating changes in the protein that amplify relaxation processes from the excited state. Above 60 °C the spectrum starts to broaden. From the spectral changes, the T_m for Ca-bound protein is estimated to be ~75 °C, corroborating our DSC results and also consistent with the data reported by Permyakov et al. (1987). In the case of the Ca-free protein, the intensity at the lowest temperature is less than 50% that of the Ca-bound protein, and it is then seen to decrease gradually as temperature rises. At intermediate Ca^{2+} saturation, the transition is not a simple average of the Ca-bound and free species but shows an intermediate transition, consistent with a dynamic equilibrium between the two forms, as reported by DSC (Filimonov et al., 1978) and phosphorescence (Sudhakar et al., 1995).

Infrared Spectroscopy. The mid-IR absorbance for parvalbumin in D_2O is shown in Figures 6 and 7 for the Ca-

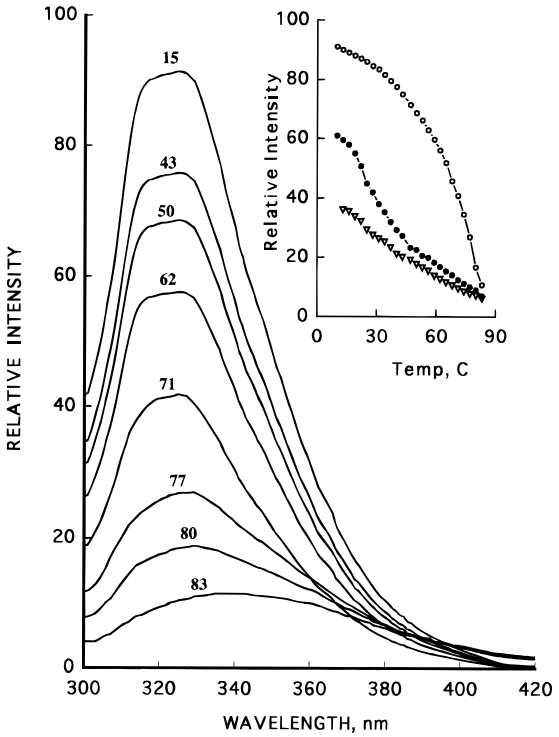

FIGURE 5: Fluorescence emission spectra of Ca-parvalbumin as a function of temperature. Buffer conditions are given in Figure 2. The excitation wavelength was 280 nm; the band-pass was 2 nm. Inset: Fluorescence intensity of Ca-bound (○), Ca-half-saturated (●), and Ca-depleted parvalbumin (▽).

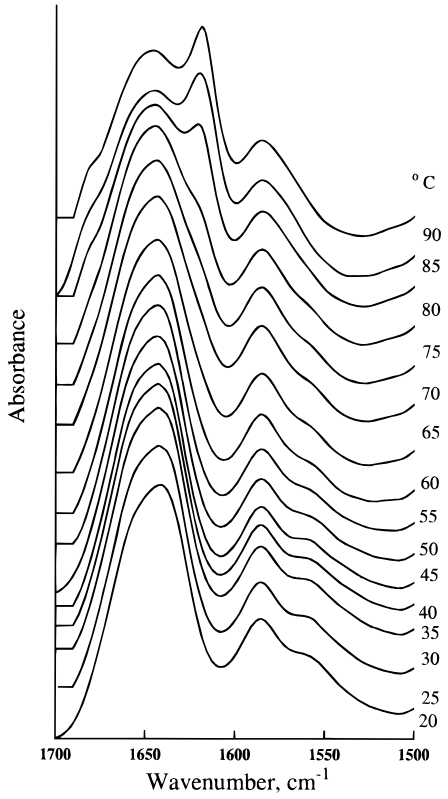

FIGURE 6: Mid-IR spectrum of Ca-parvalbumin: parvalbumin, 4.5 mM, in 10 mM sodium phosphate, 100 mM sodium chloride, and D_2O at pD 7.0. Data are sucessive spectra of the same sample taken at the temperatures indicated, starting at the lowest temperature.

bound and free proteins, respectively, at the temperatures indicated on the figures. The spectrum for Ca-parvalbumin

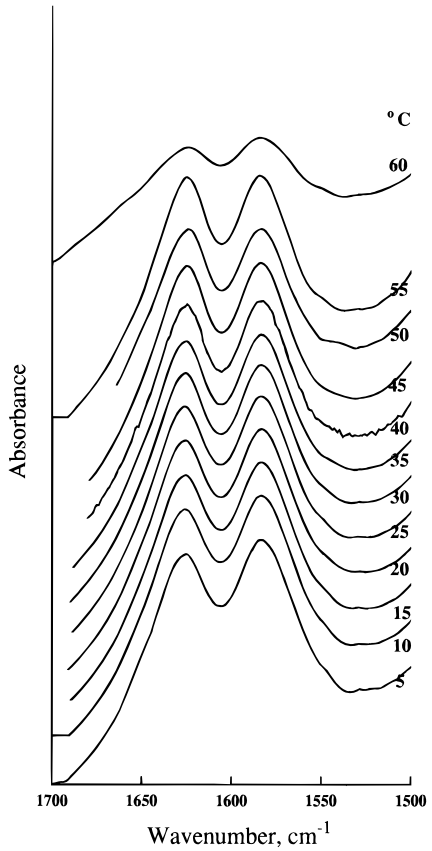

FIGURE 7: Mid-IR spectrum of Ca-free parvalbumin. The removal of Ca was achieved by addition of EGTA and monitored by the fluorescence emission. Other conditions are given in Figure 6.

is very similar to that observed for the Ca-bound pike protein by Nara et al. (1994). The peak maximum of the amide I′ region is at 1645 cm^{-1} for the Ca-bound form (Figure 6).

A broad peak centered at 1582 cm^{-1} is seen in the spectrum of both protein forms. It is assigned to the antisymmetric stretch of the COO^- groups of the parvalbumin Asp residues not coordinated to calcium (Nara et al., 1994). We also observe a shoulder at 1555 cm^{-1}. Previous work has it assigned to the COO^- groups in bidentate ligation with calcium (Deacon & Phillips, 1980; Nara et al., 1994). We confirm this assignment since we observe its disappearance in the Ca-free parvalbumin spectrum (cf. Figure 7). The X-ray analysis of carp parvalbumin (Kumar et al., 1990) shows two Ca^{2+} ions bound to six residues on the protein: the Ca in the CD site is ligated to Asp51, Asp53, Ser55, Phe57, Glu59, and Glu62 (bidentate). In the EF site the Ca is ligated to Asp90, Asp92, Asp94, Lys96, Glu101, and to a water. In the CD site, calcium has bidentate ligation with Glu62 and with Glu101 in the EF site. The 1555 cm^{-1} shoulder thus reflects coordination to these two residues. As temperature increases, the intensity of this shoulder decreases relative to the peak at 1582 cm^{-1}. This is illustrated for several temperatures on Figure 8A, and the ratio of these two peaks is plotted as a function of temperature on Figure 8B. The temperature profile shows discontinuity in the range where other indications show thermal unfolding, i.e., ∼60 °C.

Referring back to Figure 6, it can be seen that at the highest temperatures (i.e., >80 °C) a peak at 1620 cm^{-1} and a shoulder at 1684 cm^{-1} appear. These frequencies are characteristic of β sheet found in aggregated, denatured

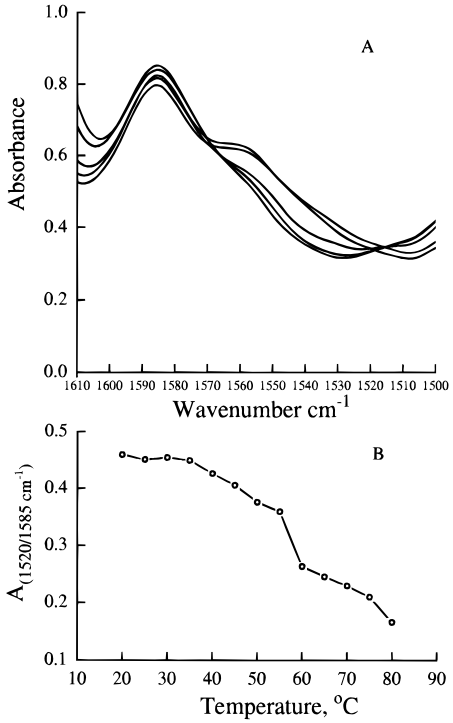

FIGURE 8: (A) Data from Figure 6 plotted on an expanded scale. Temperatures are 15, 25, 45, 55, and 65 °C from top to bottom at 1560 cm^{-1}. (B) The absorbance ratio ($A_{1520-1520}/A_{1585-1520\ cm^{-1}}$) is plotted as a function of temperature.

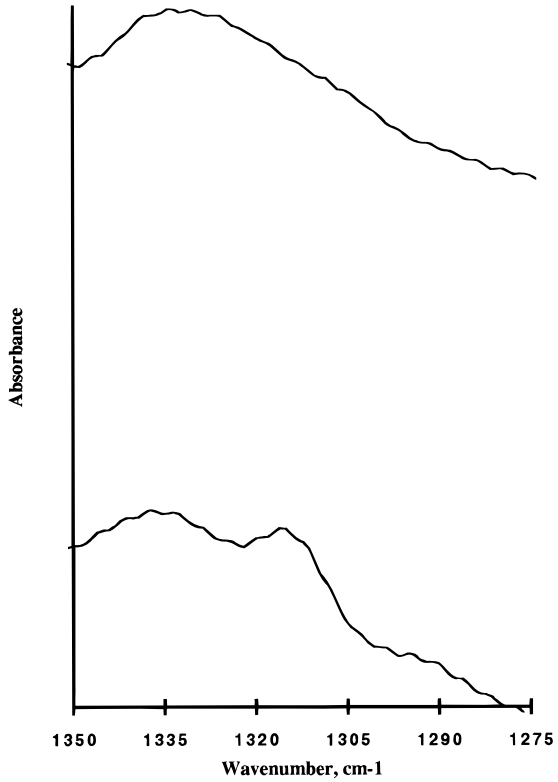

FIGURE 9: Amide III′ region of Ca^{2+}-bound (bottom) and Ca-free parvalbumin (top). Conditions are given in Figures 6 and 7, respectively.

protein (Clark et al., 1981; Ismail et al., 1992), and they also have been seen in other aggregated proteins (Holzbaur et al., 1996). The appearance of these peaks was observed to be concentration-dependent: at 10-fold lower concentration of protein, they were not observed under the same other conditions. Unlike the shoulder at 1555 cm^{-1}, the peak at 1620 cm^{-1} was irreversible and remained when the temperature was lowered. Therefore, in the mid-IR range two temperature-dependent effects are seen: the loss of Ca binding due to thermal unfolding and at higher temperatures irreversible aggregation.

The difference in the IR spectrum in the amide regions of the Ca-bound and Ca-free forms is quite striking. In the Ca-free protein (Figure 7), the amide I′ stretch is shifted some 10 cm^{-1}—to 1635 cm^{-1}. This is not unexpected: perturbation of secondary structure could result in a shift to lower frequency due to increased C═O/N−H bond indexes. Previous work has also correlated lower amide I′ frequencies with unusual helical structures (Jackson et al., 1991). The COO^- antisymmetric stretch (1582 cm^{-1}) lacks the Ca^{2+}-ligation marker band observed at 1555 cm^{-1} in Ca-parvalbumin (cf. Figure 7). The amide II′ region remains relatively unaffected by Ca removal but not so the amide III′ region (Figure 9) in which we observe complete disappearance of the Ca^{2+}-ligation marker band seen at 1316 cm^{-1} in the Ca-bound form (Figure 9). While of relatively small intensity, the region exhibits bands known to be sensitive to calcium binding. In the presence of Ca^{2+}, we observe two bands at ca. 1334 and 1316 cm^{-1}, the latter recently associated with a calcium-binding induced increase in helical structure (Fu et al., 1994).

We considered the possibility that some of the differences in the amide regions could be due to different equilibration with D_2O between the more rigid Ca-bound protein and the looser Ca-free parvalbumin. However, the spectra obtained remained constant in time over a period of time between ∼ 30 min and ∼24 h. Furthermore, addition of Ca to the calcium-free protein that was incubated in D_2O resulted in an IR spectrum in which the peak position of the amide I′ region was the same as shown in Figure 7, and the shoulder at 1570 cm^{-1}, attributed to Ca-bound carboxyls, reappeared. We did notice that the amide I′ peak showed asymmetry with extra width at higher frequency (see Figure 6) and that after cycling in D_2O from the Ca-free to the Ca-bound form some intensity was lost in the high region side (data not shown). Therefore, the absorption in the amide I′ region of the Ca-bound form may contain some contribution from unexchanged H atoms in the peptide linkage, since shifts on the order of ∼5 cm^{-1} are known to occur with D−H exchange (Arrondo et al., 1993).

Molecular Dynamics Analysis. MDS simulations of Ca-bound and Ca-free parvalbumin were performed to investigate the effect of calcium removal on the overall structure of the protein. The stability of the trajectories was assessed by monitoring the potential energy and the rms deviation from the X-ray coordinates. A representative evolution of the potential energy with time is shown in Figure 10 for the solvated Ca-free parvalbumin. Following the warm-up phase, the potential energy is seen to remain fairly constant in the last 140 ps of simulation. The solvated results are consistent with the last 60 ps of the distance-dependent dielectric simulation. Figure 11 illustrates the structural changes associated with calcium removal. Consistent with the experimental spectroscopic studies, removal of calcium results in significant perturbation of the α-helical structure at the end of the simulation (Figure 11B). Some helical character is conserved, however: helix A loses one of its three turns, helix B has one of its two turns severely distorted, helix C loses one of its three turns and has the other distorted,

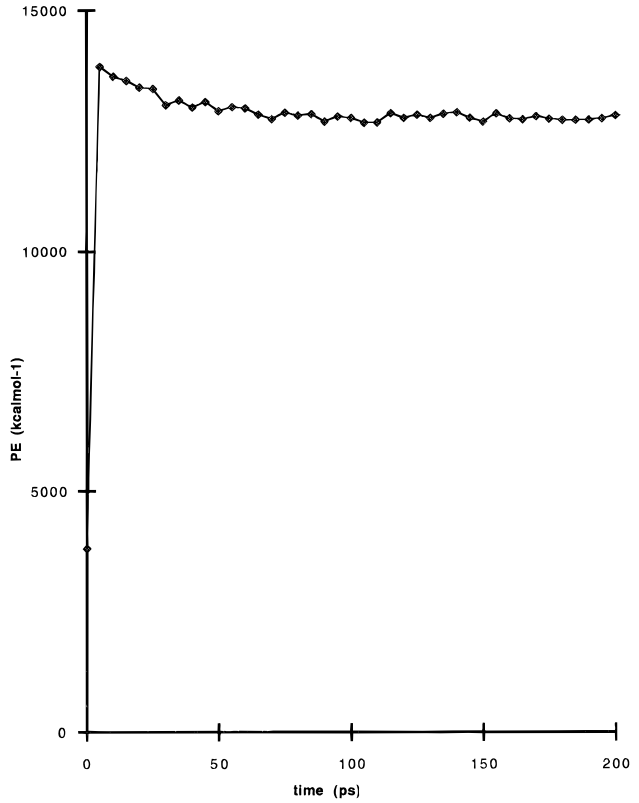

FIGURE 10: Time course evolution of the total potential energy of the calcium-depleted solvated parvalbumin.

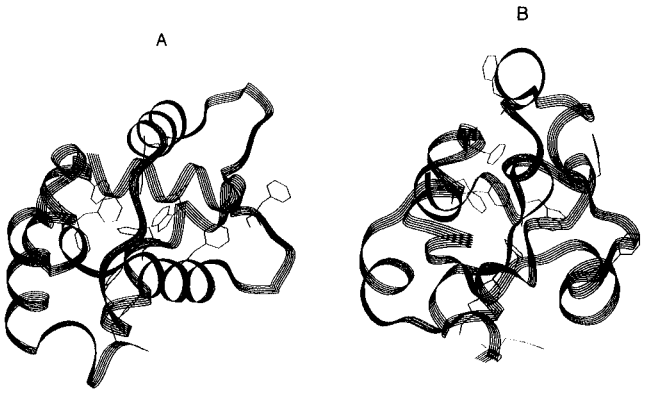

FIGURE 11: Three-dimensional structures of Ca-free cod parvalbumin: (A) starting structure after Ca removal and minimization; (B) structure after 120 ps of MDS.

helix D maintains its two turns but in a looser configuration, helix E loses one of its three turns, and the last helix, F, likewise has one of its two turns removed. Figure 12 shows that, in the case of the Ca-bound simulation, helical perturbations are minimal: all helices are clearly preserved and the protein undergoes no significant rearrangement.

DISCUSSION

Parvalbumin is a particularly clear illustration of the general principle: substrate or cofactor binding increases protein stability when the binding is tighter to the folded form. In the case of parvalbumin, changes throughout all protein regions occur upon calcium binding (Figure 11). Simulations showed that a new structure is obtained within approximately 60 ps after Ca removal. We discuss below whether the new structure is consistent with experimental results.

The major effect of Ca removal in the simulated model is a decrease in the α-helical content. A CD spectrum is representative of the asymmetry of the optical center, and CD has been exhaustively used to monitor changes in the secondary and tertiary structure of proteins (Yang et al., 1986; Johnson, 1990) and polypeptides (Cascio & Wallace, 1995). In the far-UV region, CD monitors transitions assigned to peptide chromophores sensitive to secondary structural changes, and in the near-UV region, CD reflects changes occurring in the aromatic chromophore transitions. The ellipticity at 222 nm is commonly used as an α-helical determinant (Johnson, 1990; Hirst & Brooks, 1994). The observed ellipticity changes are indicative of a lower α-helical content in the Ca-free protein (50% of the Ca-bound α-helical structure is retained in the Ca-free protein). The modeled Ca-free structure (Figure 11) also shows approximately the same reduction in helical structure and is thus in very good agreement with experimental results. Other CD (White, 1988; Hutnik et al., 1990) and NMR (Cave et al., 1979) studies have also shown that Ca^{2+}-free parvalbumin retains some secondary structure.

A further indication of helical structure is provided by infrared spectroscopy. FTIR spectroscopy is now increasingly used as a probe of secondary structure (Goormaghtigh et al., 1994), especially in the amide stretch region. The amide I′ vibrational region is mostly monitored because protein absorption is usually intense within its range (1600−1700 cm^{-1}). It corresponds to C═O stretches weakly coupled to C−N stretches and N−H bending modes. In a deuterated solvent, the amide II′ region (1500−1600 cm^{-1}) displays absorption assigned to C−N stretches strongly coupled to N−H bending. The amide III′ region features weaker absorption in the 1200−1350 cm^{-1} range, assigned to N−H in-plane bending modes coupled to C−N stretches and C−H/N−H deformation modes (Fu et al., 1994). FTIR has been applied to secondary structure analysis for several Ca-binding proteins including parvalbumin for which Ca−, Mg−, and Mn−ligand interactions have been correlated to marker bands indicative of the coordination of the metal site (Nara et al., 1994). FTIR has also been used to investigate the α-helical structure of frog parvalbumin (Jackson et al., 1991). The IR of the amide I′ region is drastically changed upon Ca removal (Figures 7 and 8), as is the amide III′ region (Figure 9). The positions of the amide regions depend strongly on the local environment; for instance, an anomalously high amide I frequency is usually attributed to a distorted α-helix (Rothschild & Clark, 1979; Krimm & Dwivedi, 1982; Dwivedi & Krimm, 1984). Since the simulations show that throughout the whole structure H bonding is decreased upon Ca removal, the overall shifts in the amide regions are thus not surprising.

FTIR also provides more specific indications of the changes occurring with Ca binding. Variations in the COO^- stretch are Ca dependent, and the spectra clearly show that an increase in temperature causes the release of Ca. Protein stability is known to be a complex function of a variety of factors including shifts in both ionization and hydrophobic interactions as temperature is changed (Privalov et al., 1986; Privalov, 1990). The major ligating species is carboxyl, and the solubility of its Ca salts increases with temperature. For instance, the solubility of $CaCO_3$ in g/100 mL is 0.0014 at 25 °C and 0.0019 at 75 °C, and for Ca succinate these values are 0.19 at 10 °C and 0.89 at 80 °C (Weast & Astle, 1982,

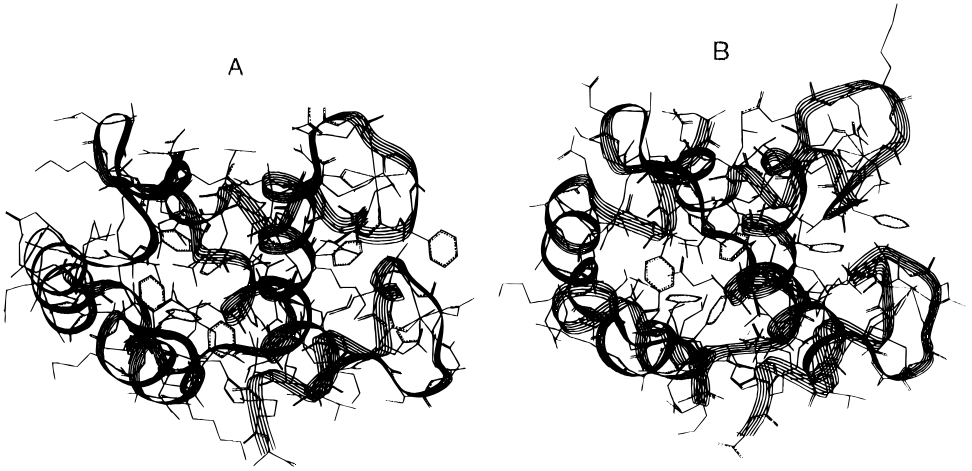

FIGURE 12: Three-dimensional structures of Ca-bound cod parvalbumin: (A) starting structure after minimization; (B) structure after 200 ps of MDS.

1983). Examination of the structure of Ca-parvalbumin (Figure 1) shows that residues from each of the two helices and the loop region form bonds with the metal. The binding of Ca then serves as a major factor in the folding of the protein and its stability.

The FTIR spectra also show that loss of Ca from the protein and irreversible aggregation are two separate processes. The aggregation continues to increase at the highest temperature, whereas the shoulder at 1550 cm^{-1} shows loss of Ca (Figure 6) in the same temperature range in which DSC shows a thermal transition (Figure 4).

The luminescence from Trp represents an extensively studied spectroscopic marker; the first fluorescence work on cod parvalbumin showed that Ca^{2+} removal was accompanied by a conformational change which, for type III isoprotein from cod, resulted in changes of the intrinsic fluorescence of its single Trp, thus showing that this residue became exposed (Permyakov et al., 1980). Spectral shifts and changes in fluorescence lifetime and anisotropy (Ferreira, 1989; Hutnik et al., 1990), fluorescence quenchability (Castelli et al., 1988; Eftink & Wasylewski, 1989), and phosphorescence lifetime (Sudhakar et al., 1995) all indicate changes between the Ca-bound and Ca-free forms. For the modeled protein in the Ca-bound form, the Trp is buried, while in the Ca-free protein, the indole orientation flips; it is tilted toward the peptide chain in the Ca-bound form and away in the free form (Figure 11). These results are consistent with the spectral shifts shown in Figure 2 and the other spectroscopic indications of Trp found in the literature.

The data presented in this work are consistent with the literature evidence showing that the binding of Ca increases protein stability. The stability of parvalbumin to denaturation by heat (Filimonov et al., 1978) and its structural flexibility—as measured by room temperature phosphorescence—were additionally shown to be very sensitive to the binding of Ca^{2+} ions (Sudhakar et al., 1995). In a previous transient absorption study combined with time-resolved fluorescence and phosphorescence measurements, we were able to show that the removal of calcium results in a protein that undergoes dynamic changes in the submicrosecond to millisecond time scale (Sudhakar et al., 1993a). Dynamical changes, like the structural changes, were shown to occur in all regions of the protein, as shown by comparisons of the excited triplet state behavior of Phe (Sudhakar et al., 1993b) and Trp (Sudhakar et al., 1993a). The work presented in this paper strengthens our previous conclusions and provides direct spectroscopic evidence for these dynamical changes.

Summary. The work described in this paper attempts to characterize the Ca-free structure of cod parvalbumin, focusing on whether a modeled structure of the Ca-free protein can complement structural information derived from spectroscopic data. In summary, the spectral data are consistent with the modeled parvalbumin structure as follows: the Ca-free protein shows reduced stability, increased mobility, increased exposure of Trp, and loss of helical content.

REFERENCES

Anderson, C. M., Zucker, F. H., & Steitz, T. A. (1979) *Science 204*, 375−380.
Arrondo, J. L. R., Muga, A., Castresana, J., & Goni, F. M. (1993) *Prog. Biophys. Mol. Biol. 59*, 23−56.
Barnes, N. D., Hull, D., Balgobin, L., & Gompertz, D. (1970) *Lancet 2*, 244−245.
Bernstein, F. C., Koetzle, T. F., Williams, G. J. B., Meyer, E. F., Jr., Brice, M. D., Rodgers, J. R., Kennard, O., Shimanouchi, T., & Tasumi, M. (1977) *J. Mol. Biol. 112*, 535−549.
Brandts, J. F., Hu, C. Q., Lin, L.-N., & Mas, M. T. (1989) *Biochemistry 28*, 8588−8596.
Callis, P. R. (1991) *J. Chem. Phys. 95*, 4230−4240.
Cascio, M., & Wallace, B. A. (1995) *Anal. Biochem. 227*, 90−100.
Castelli, F., White, H. D., & Forster, L. S. (1988) *Biochemistry 27*, 3366−3372.
Cave, A., Pages, M., Morin, P., & Dobson, C. M. (1979) *Biochimie 61*, 607−613.
Celio, M. R. (1990) *Neuroscience 35*, 375−475.
Clark, A. H., Saunderson, D. H. P., & Suggestt, A. (1981) *Int. J. Pept. Protein Res. 17*, 353.
Deacon, G. B., & Phillips, R. J. (1980) *Coord. Chem. Rev. 33*, 227−250.
Declercq, J.-P., Tinant, B., Parello, J., & Rambaud, J. (1991) *J. Mol. Biol. 220*, 1017−1039.
Ding, H. Q., Karasawa, N., & Goddard, W. A. (1992) *J. Chem. Phys. 97*, 4309−4320.
Dwivedi, A. M., & Krimm, S. (1984) *Biopolymers 23*, 923−943.
Eberspach, I., Strassburger, W., Glatter, U., Gerday, C., & Wollmer, A. (1988) *Biochim. Biophys. Acta 952*, 67−76.
Eftink, M. R., & Wasylewski, Z. (1989) *Biochemistry 28*, 382−391.
Ferreira, S. T. (1989) *Biochemistry 28*, 10066−10072.
Filimonov, V. V., Pfeil, W., Tsalkova, T. N., & Privalov, P. L. (1978) *Biophys. Chem. 8*, 117−122.

Fu, F.-N., DeOliveira, D. B., Trumble, W. R., Sarkar, H. K., & Singh, B. R. (1994) *Appl. Spectrosc. 48*, 1432−1441.
Gerday, C., Bolis, L., & Gilles, R. (1988) *Calcium and Calcium Binding Proteins*, Springer-Verlag, Berlin.
Goormaghtigh, E., Cabiaux, V., & Ruysschaert, J.-M. (1994) *Subcellular Biochem. 23*, 329−362.
Hagler, A. T., & Lifson, S. (1974) *J. Am. Chem. Soc. 96*, 5327−5335.
Hagler, A. T., Huler, E., & Lifson, S. (1974) *J. Am. Chem. Soc. 96*, 5319−5327.
Haiech, J., Derancourt, J., Pechere, J. F., & Demalle, J. G. (1979) *Biochemistry 18*, 2752−2758.
Harvey, S. C. (1989) *Proteins 5*, 78−92.
Henrickson, W. A., & Karle, J. (1973) *J. Biol. Chem. 248*, 3327−3334.
Hirst, J. D., & Brooks, C. L., III (1994) *J. Mol. Biol. 243*, 173−178.
Holzbaur, I. E., English, A. M., & Ismail, A. A. (1996) *Biochemistry 35*, 5488−5494.
Hori, K., Kushick, J. N., & Weinstein, H. (1988) *Biopolymers 27*, 1865−1886.
Horrocks, W. D., Jr., & Collier, W. E. (1981) *J. Am. Chem. Soc. 103*, 2856−2862.
Hutnik, C. M. L., MacManus, J. P., & Szabo, A. G. (1990) *Biochemistry 29*, 7318−7328.
Ismail, A. A., Manstsch, H. H., & Wong, P. T. T. (1992) *Biochim. Biophys. Acta 1121*, 183.
Jackson, M., Haris, P. I., & Chapman, D. (1991) *Biochemistry 30*, 9681−9686.
Jaenicke, R. (1987) *Prog. Biophys. Mol. Biol. 49*, 117−237.
Johnson, W. C. (1990) *Proteins: Struct., Funct., Genet. 7*, 205−214.
Kretsinger, R. H., & Nockolds, C. E. (1973) *J. Biol. Chem. 248*, 3313−3326.
Krimm, S., & Dwivedi, A. M. (1982) *Science 216*, 407−408.
Kumar, V. D., Lee, L., & Edwards, B. F. P. (1990) *Biochemistry 29*, 1404−1412.
Kuwajima, K. (1989) *Proteins: Struct., Funct., Genet. 6*, 87−103.
Longworth, J. W. (1971) in *Excited States of Proteins and Nucleic Acids* (Steiner, R. F., & Weinryb, I., Eds.) pp 319−484, Plenum Press, New York.
Mehler, E. L. (1990) *Protein Eng. 3*, 415−417.
Mehler, E. L., Pascual-Ahuir, J.-L., & Weinstein, H. (1991) *Protein Eng. 4*, 625−637.
Mehler, E. L., Kusnick, J. N., & Weinstein, H. (1993) *Mol. Simulation 10*, 309−334.
Nara, M., Tasumi, M., Tanokura, M., Hiraoki, T., Yazawa, M., & Tsutsumi, A. (1994) *FEBS Lett. 349*, 84−88.
Pace, C. N., & Grimsley, G. R. (1988) *Biochemistry 27*, 3242−3246.
Permyakov, E. A., Yarmolenko, V. V., Emelyanenko, V. I., Burstein, E. A., Closset, J., & Gerday, C. (1980) *Eur. J. Biochem. 109*, 307−315.
Permyakov, E. A., Kalinichenko, L. P., Medvedkin, V. V., Burstein, E. A., & Gerday, C. (1983) *Biochim. Biophys. Acta 749*, 185−191.
Permyakov, E. A., Ostrovsky, A. V., & Kalinichenko, L. P. (1987) *Biophys. Chem. 28*, 225−233.
Persson, E., & Petersen, L. C. (1995) *Eur. J. Biochem. 234*, 293−300.
Privalov, P. L. (1990) *Crit. Rev. Biochem. Mol. Biol. 25*, 281−305.
Privalov, P. L., Griko, Y. V., Venyaminov, Y., & Kutyshenk, V. P. (1986) *J. Mol. Biol. 190*, 487−498.
Roquet, F., Declercq, J.-P., Tinant, B., Rambaud, J., & Parello, J. (1992) *J. Mol. Biol. 223*, 705−720.
Rothschild, K. J., & Clark, N. A. (1979) *Science 204*, 311−312.
Schmidt, K. E., & Lee, M. A. (1991) *J. Stat. Phys. 63*, 1223−1237.
Solmajer, T., & Mehler, E. L. (1991) *Protein Eng. 4*, 911−917.
Sudhakar, K., Phillips, C. M., Williams, S. A., & Vanderkooi, J. M. (1993a) *Biophys. J. 64*, 1503−1511.
Sudhakar, K., Wright, W. W., Williams, S. A., Phillips, C. M., & Vanderkooi, J. M. (1993b) *J. Fluoresc. 3*, 57−64.
Sudhakar, K., Phillips, C. M., Owen, C. S., & Vanderkooi, J. M. (1995) *Biochemistry 34*, 1355−1363.
Sugawara, T., Kuwajima, K., & Sugai, S. (1991) *Biochemistry 30*, 2698−2706.
Weast, R. C., & Astle, M. M. (1982−1983) *CRC Handbook of Chemistry and Physics*, CRC Press, Inc., Boca Raton, FL.
White, H. D. (1988) *Biochemistry 27*, 3357−3365.
Yang, J. T., Wu, C.-S. C., & Martinez, H. M. (1986) *Methods Enzymol. 130*, 208−269.

BI962436Q